Title

Arterial spin labeling perfusion MRI in the Alzheimer's Disease Neuroimaging Initiative: Past, present, and future

Journal

Alzheimer's & Dementia, 20(12)

ISSN

1552-5260

Authors

Thropp, Pamela

Phillips, Eliana

Jung, Youngkyoo

et al.

Publication Date

2024-12-01

DOI

10.1002/alz.14310

Peer reviewed

Received: 30 April 2024 | Accepted: 11 September 2024

DOI: 10.1002/alz.14310

Alzheimer's & Dementia®
THE JOURNAL OF THE ALZHEIMER'S ASSOCIATION

REVIEW ARTICLE

Arterial spin labeling perfusion MRI in the Alzheimer's Disease Neuroimaging Initiative: Past, present, and future

Pamela Thropp[1] | **Eliana Phillips**[1] | **Youngkyoo Jung**[2] | **David L. Thomas**[3] | **Duygu Tosun**[4] | **for the Alzheimer's Disease Neuroimaging Initiative**

[1]Department of Veterans Affairs Medical Center, Northern California Institute for Research and Education (NCIRE), San Francisco, California, USA

[2]Department of Radiology, University of California Davis, Sacramento, California, USA

[3]Department of Brain Repair and Rehabilitation, UCL Queen Square Institute of Neurology, London, UK

[4]Department of Radiology and Biomedical Imaging, University of California San Francisco, San Francisco, California, USA

Correspondence
Duygu Tosun, Department of Radiology and Biomedical Imaging, University of California San Francisco, 4150 Clement Street, Bldg 13 114 M, San Francisco, CA 94121, USA.
Email: duygu.tosun@ucsf.edu

Data used in preparation of this article were obtained from the Alzheimer's Disease Neuroimaging Initiative (ADNI) database (adni.loni.usc.edu). As such, the investigators within the ADNI contributed to the design and implementation of ADNI and/or provided data but did not participate in the analysis or writing of this report. A complete listing of ADNI investigators can be found at: http://adni.loni.usc.edu/wp-content/uploads/how_to_apply/ADNI_Acknowledgement_List.pdf.

Funding information
National Institutes of Health, Grant/Award Number: U19AG024904

Abstract

On the 20th anniversary of the Alzheimer's Disease Neuroimaging Initiative (ADNI), this paper provides a comprehensive overview of the role of arterial spin labeling (ASL) magnetic resonance imaging (MRI) in understanding perfusion changes in the aging brain and the relationship with Alzheimer's disease (AD) pathophysiology and its comorbid conditions. We summarize previously used acquisition protocols, available data, and the motivation for adopting a multi-post-labeling delay (PLD) acquisition scheme in the latest ADNI MRI protocol (ADNI 4). We also detail the process of setting up this scheme on different scanners, emphasizing the potential of ASL imaging in future AD research.

KEYWORDS
Alzheimer's disease, arterial spin labeling, arterial transit time, cerebral blood flow, magnetic resonance imaging, multiple post-label delay

Highlights

- The Alzheimer's Disease Neuroimaging Initiative (ADNI) adopted multimodal arterial spin labeling magnetic resonance imaging (ASL MRI) to meet evolving biomarker requirements.
- The ADNI provides one of the largest multisite, multi-vendor ASL data collections.
- The ADNI 4 incorporates multi-post-labeling delay ASL techniques to jointly quantify cerebral blood flow and arterial transit time.
- ADNI 4 ASL MRI protocol is apt for detecting early Alzheimer's disease with cerebrovascular pathology.

1 | BACKGROUND

Since its inception two decades ago, the Alzheimer's Disease Neuroimaging Initiative (ADNI) has been instrumental in transforming our understanding of Alzheimer's disease (AD), the most common form of neurodegenerative dementia. Primary objectives of the ADNI have included the development of standardized neuroimaging protocols that have been widely used in clinical trial study designs and multimodality imaging data repositories to investigate disease progression and validate biomarkers for use in clinical trials. The ADNI has also been dedicated to evaluating the potential of novel imaging techniques in these contexts. One such technique is arterial spin labeling (ASL) perfusion imaging, a magnetic resonance imaging (MRI) method that offers critical insight into cerebral perfusion dynamics, which are significantly altered in AD.[1–29] ASL has served as one of the non-invasive functional brain imaging modalities in the ADNI, facilitating assessment of brain function by means of cerebral blood flow (CBF). ASL MRI complements both structural MRI methods and molecular positron emission tomography (PET) by offering insights into perfusion changes linked to core biomarkers of AD. For instance, lower CBF in temporo-parietal regions has been linked to amyloid beta (Aβ) accumulation as measured by amyloid PET imaging and shown to be predictive of presence of amyloid pathology in early disease stages.[3,7] Studies have provided evidence that pathologic tau is a major correlate of CBF in early Braak stages, independent of amyloid, apolipoprotein E (*APOE*) genotype, and small vessel disease markers.[15,18,30] This finding suggests a synergy between tau pathology and cerebral perfusion independent of amyloid deposition, and that ASL-MRI might offer unique insights into the vascular and neurodegenerative processes occurring in AD, independent of other known risk factors. Furthermore, multimodality imaging studies suggest that changes in CBF as a surrogate biomarker of vascular dysregulation might precede detectable AD pathological changes.[9,19,22,25] Further research is needed to fully understand the role of ASL MRI measures in AD diagnosis and monitoring, but current evidence supports its complementary role in a more comprehensive understanding of AD pathophysiology. In addition, the revised criteria for diagnosis and staging of AD from the Alzheimer's Association Workgroup[31] acknowledge biomarkers that are not specific to AD pathology but are important in the AD pathogenic pathways. Additionally, the revised criteria describe the importance of integration of common co-pathologies, such as cerebrovascular disease, as they modify relationships between clinical and biological AD stages. Therefore, although regional CBF changes might not be specific to AD, ASL MRI fits well into the revised staging criteria by providing valuable information on vascular physiology and neurodegeneration, allowing for a more comprehensive understanding of an individual beyond or in addition to the presence of AD pathology, ultimately leading to improved diagnostic and therapeutic strategies.

ASL MRI is a perfusion imaging technique that leverages magnetically labeled arterial blood water as an endogenous tracer.[32–34] After a specific post-labeling delay (PLD) period, during which the labeled blood travels from the labeling location to the imaging region, brain images are acquired. These images can then be used to calculate and map the blood flow within the brain.[35] Before the introduction of ASL-MRI, measurements of CBF were typically made using PET with injections of radiolabeled water. ASL-MRI is non-invasive, without radioactive exposure, is easily co-registered to structural MRI, and data can be acquired in < 10 minutes.[32–34,36–38] ASL-MRI and ^{18}F-fluorodeoxyglucose PET (FDG PET) have been successfully used to study overlapping alterations that occur in AD,[39,40] connecting CBF with metabolism and providing insight into the overall integrity of neurovascular coupling in the brain. Before the incorporation of ASL MRI into the ADNI study, an increasing body of work showed that the method can detect regional patterns of reduced brain perfusion in AD[41,42] and even those with mild cognitive impairment (MCI).[41] In addition, MCI and AD present a characteristic pattern of reduced perfusion that is different from the perfusion pattern of other dementias, such as frontotemporal dementia (FTD).[41–43] Moreover, it has been shown that alterations in brain atrophy and perfusion in AD can be discordant,[41] implying that ASL MRI provides information complementary to structural MRI. Altogether, along with dependable repeatability,[44] this evidence supported ASL MRI as an ideal candidate technique for longitudinal studies aimed at understanding neural function, pathophysiology, and progression of AD.

Concurrently, there was a growing need for more sensitive detection methods capable of identifying subtle and early treatment signals, as trials moved into the preclinical phase of AD. Moreover, the demand for additional functional imaging techniques began to increase in trial

RESEARCH IN CONTEXT

1. **Systematic review**: This sweeping review was conducted by members of the Alzheimer's Disease Neuroimaging Initiative (ADNI) magnetic resonance imaging (MRI) Core to map use and protocol optimization of arterial spin labeling (ASL) MRI as a functional imaging biomarker of pathophysiological changes associated with Alzheimer's disease (AD) pathology and disease progression.
2. **Interpretation**: The incorporation and expansion of ASL in the ADNI has proven invaluable in enhancing our understanding of brain blood perfusion changes in the aging brain and their relationship with AD pathophysiology and comorbid conditions. Through more precise and comprehensive cerebral blood flow (CBF) measurements, multiple post-labeling delays (multi-PLD) techniques hold promise in advancing our understanding of AD and its common comorbid condition, cerebrovascular disease.
3. **Future directions**: Incorporation of multi-PLD ASL techniques into the ADNI 4 imaging protocol provides more accurate estimates of CBF changes when investigating early stages of AD, as well as providing complementary information relating to abnormal arterial transit times intertwined with cerebrovascular pathology.

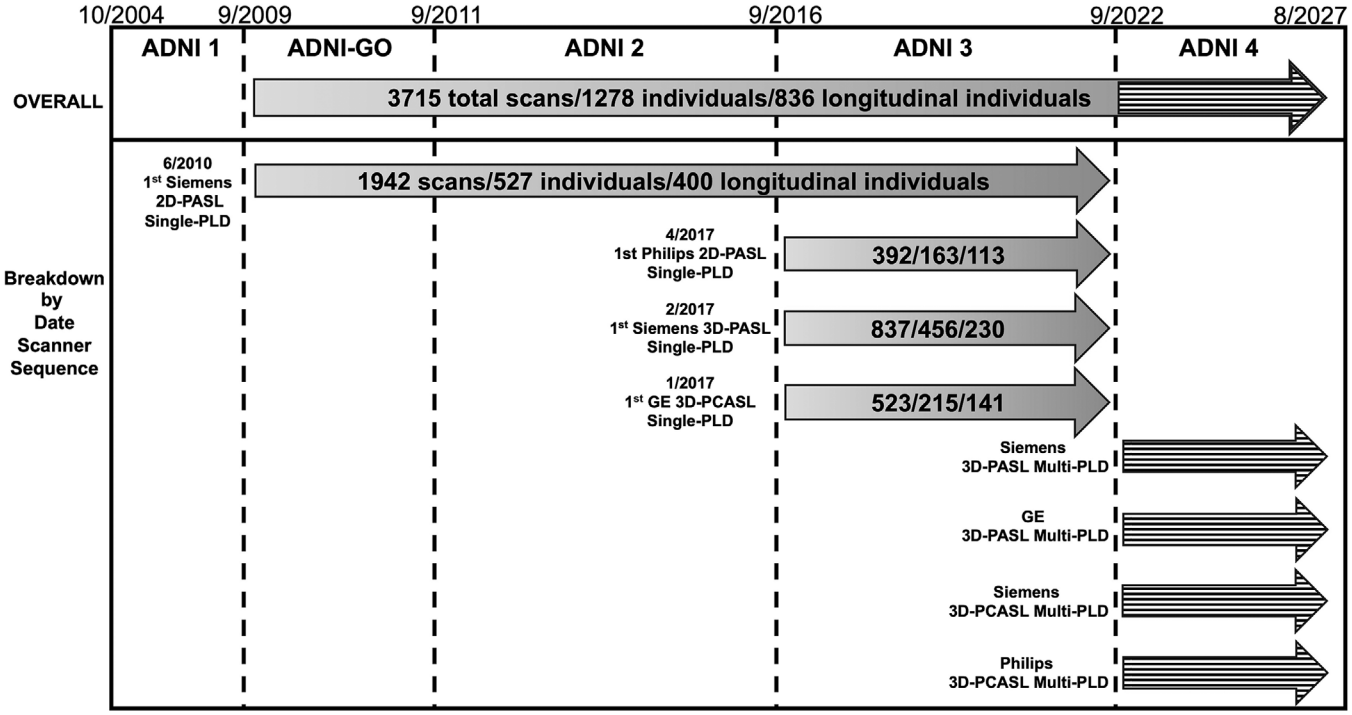

FIGURE 1 Timeline of ASL MRI acquisition types used in the ADNI. ADNI study cycle boundaries (1–4) are indicated by dates across the top and dashed vertical lines. The top arrow summarizes the total number of scans, individuals, and longitudinal individuals who have ASL MRI data. Each subsequent arrow represents a different vendor and acquisition type with a label to the left including the date of the first scan. Numbers within each arrow indicate the # scans/# unique individuals/# individuals with longitudinal data available, as of April 2024. Longitudinal individuals have had more than one scan since 2010. Striped arrows refer to ongoing recruitment and acquisitions in ADNI 4. ADNI, Alzheimer's Disease Neuroimaging Initiative; ASL, arterial spin labeling; MRI, magnetic resonance imaging; PASL, pseudo-arterial spin labeling; PCASL, pseudo-continuous arterial spin labeling; PLD, post-labeling delay.

protocols, aimed at providing a more comprehensive assessment of treatment effects. In tandem with the evolving biomarker requirements of AD clinical trials, the ADNI adapted a multimodality MRI approach, which included ASL MRI.

As shown by the timeline illustrated in Figure 1, the single-vendor substudy of ASL MRI was initially launched during the ADNI GO cycle and continued into the ADNI 2 cycle. This study was later expanded to include all of the ADNI sites, regardless of the MRI scanner vendor, resulting in one of the largest multisite, multi-vendor ASL MRI data collections within the scope of AD and related disorders. In these early years of ADNI ASL imaging, single PLD ASL MRI protocols were used. While these protocols offered significant insights into the cerebral perfusion abnormalities in AD, they also had limitations. The most significant of these was the inability to accurately quantify CBF in regions with delayed arterial transit times (ATT). This limitation led to the exploration of multi-PLD ASL MRI protocols. This approach, which captures multiple time points after blood bolus labeling, allows for better characterization of the arterial inflow curve and more accurate quantification of CBF across different vascular territories.[45,46] This is particularly relevant for AD research, as elderly individuals and AD patients often exhibit both altered perfusion and extended vascular transit times.

This paper aims to provide an overview of the journey of ASL-MRI in the ADNI. We begin by summarizing the protocols used earlier and the data derived from them. We then delve into the motivation behind the adoption of the multi-PLD acquisition scheme and describe the process of setting up this advanced technique across different MRI scanners. Further, we highlight the potential role of multi-PLD ASL MRI in understanding the complex pathophysiology of AD and its comorbid conditions, particularly cerebrovascular disease.

2 | ASL IN THE ADNI: THE PAST

ASL MRI was first incorporated into the ADNI study during the ADNI GO cycle in 2009. During this period, the leading-edge ASL MRI acquisition method was 2D ASL using multi-slice echo-planar imaging (EPI) readout, implemented on 3 Tesla (3T) Siemens scanners. However, it was not feasible to conduct a multi-vendor ASL MRI study with a unified acquisition sequence across various platforms. The complexity of a multi-vendor ASL MRI study encompassed differences in hardware and sequence implementations across scanners, as well as varying acquisition protocols. These factors could introduce variability in the ASL MRI signal and the physiological modeling of CBF, posing challenges in ensuring consistency of CBF quantification across different platforms. Consequently, an ASL MRI sequence was added exclusively for subjects imaged on Siemens 3T Trio and Verio scanners using uniform product sequences, thereby producing comparable data across sites.

TABLE 1 Single PLD ASL MRI acquisition types used in ADNI GO/2/3 cycles.

	Siemens 2D PASL (ADNI GO/2/3)	Siemens 3D PASL (ADNI 3)	Philips 2D PASL (ADNI 3[b])	GE 3D pCASL (ADNI 3)
Software versions	20VB17	Prisma 20180612 Prisma D13 Prisma VE11C Skyra E11 Skyra VE11 Magento Vida-XT	R3, R5	25 ×, widebore 25 ×
TR	3400 ms	4000 ms	5000 ms	4888 ms
TE	12 ms	20.26-21.80 ms	16 ms	10.528 ms
Field of view	256 × 256 mm^2	240 × 240 mm^2	192 × 192 mm^2	240 × 240 mm^2
Acquisition matrix	64 × 64	64 × 64	64 × 64	128 × 128
Reconstruction matrix	64 × 64	128 × 128	64 × 64	128 × 128
Slice thickness	4 mm	4.5 mm	4 mm	4 mm
Tag thickness	100 mm	N/A	130 mm	N/A
Number of slices	24	N/A	40	N/A
Bandwidth	2368 Hz/pix	2442–2604 Hz/pix	1567.9–1794.2 Hz/pix	976.6 Hz/pix
Background suppression	Yes	Yes	Yes	Yes
M0 available	Yes	No	No	Yes
Control-tag pairs available	Yes	Yes	Yes	No[a]
Mode/readout	PICORE, Q2TIPS	GRASE	EPISTAR	Stack of spirals
Bolus duration	700 ms	800 ms	700 ms	1800 ms
Inversion time/PLD	1200 ms	2000 ms	2000 ms	2025 ms
Number of repeats	54	10	30	3
Acquisition time	6:02 min	5:24–8:04 min	5:10 min	6 min
Number of arms	N/A	N/A	N/A	8
Number of points per arm	N/A	N/A	N/A	512

Abbreviations: ADNI, Alzheimer's Disease Neuroimaging Initiative; ASL, arterial spin labeling; MRI, magnetic resonance imaging; PASL, pseudo- arterial spin labeling; pCASL, pseudo-continuous arterial spin labeling; PLD, post-labeling delay; TE, echo time; TR, repetition time.
[a]Provided as vendor estimated perfusion-weighted tag—control difference images.
[b]Although 3D pCASL was planned to be acquired on Philips systems upgraded to version 5.3, none of the ADNI Philips systems were upgraded to version 5.3 during the ADNI 3 study cycle.

The ASL imaging substudy conducted at select 3T Siemens ADNI GO sites aimed to demonstrate the feasibility of ASL MRI in a multisite setting and compare the findings to FDG PET. The ASL MRI substudy was extended into the ADNI 2 cycle, starting in 2011 and continuing until 2017. Specifics of ADNI GO/2 ASL MRI acquisition protocol are summarized in Table 1.

The decision to select a specific PLD was driven by the need to optimize imaging for elderly participants, both with and without cognitive impairment, who fall within the age range studied in the ADNI. Specifically, it was found that a minimum of TI2 of 1800 ms was needed in an elderly population to minimize intravascular signal contamination in the ASL images.[47] Given that CBF and ATT can vary with age and disease status, the chosen PLD aimed to accommodate these variations, ensuring sufficient time for labeled blood to reach the imaging slices.[47] When the ADNI started, single-PLD imaging was prevalent mainly due to its relatively short acquisition time, making it a practical choice for the study. As such, the selection of this PLD was a balance between optimizing signal-to-noise ratio (SNR) for CBF measurement and minimizing sensitivity to ATT effects, while considering the overall acquisition time constraints.[34]

Although restricted to Siemens-only sites (15 and 23 sites during the ADNI GO and ADNI 2 cycles, respectively), the integration of ASL MRI into ADNI GO and subsequently ADNI 2 represented a significant stride in the endeavor to evaluate the feasibility of multisite ASL imaging at such a large scale. Around this time, the International Society for Magnetic Resonance in Medicine Perfusion Study Group published a consensus paper on recommended harmonized sequences and protocols for ASL MRI in the brain,[34] and other studies also investigated

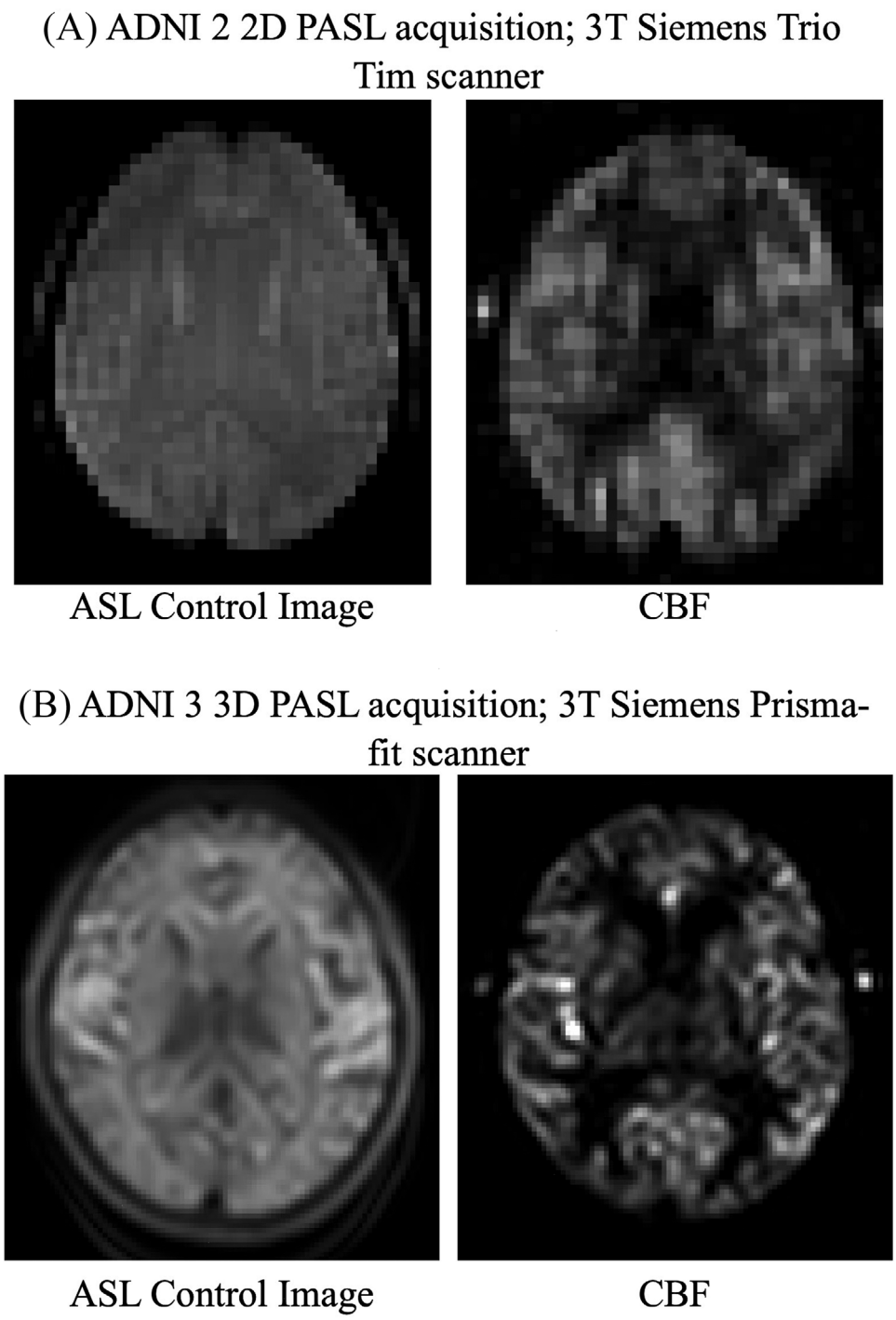

FIGURE 2 Single-PLD Siemens PASL acquisitions from a cognitively unimpaired 77-year-old female subject illustrating quality improvement from 2D to 3D ASL MRI acquisitions. CBF is presented in mL/100 g/min. ASL MRI data were acquired 2 years apart. ASL, arterial spin labeling; CBF, cerebral blood flow; MRI, magnetic resonance imaging; PASL, pseudo-arterial spin labeling; PLD, post-labeling delay.

the intrinsic sources of inter-scanner variability for multisite ASL MRI.[48] In 2017, with the start of the ADNI 3 cycle, ASL MRI acquisition was expanded to incorporate all three major MRI vendors (Siemens, GE, and Philips) across all the ADNI sites. This expansion was driven by the primary objective of the ADNI to validate biomarkers for clinical trials, which typically involve clinical imaging sites operating with a diverse range of MRI vendors and models. Although this introduced the complexity of having multiple "varieties" of ASL MRI data in the ADNI 3 dataset, the step was crucial in addressing the heterogeneity typically encountered in large multicenter studies and clinical trials.

The expanded ASL MRI acquisition in the ADNI 3, summarized in Table 1, also provided an opportunity to compare the effect size of CBF metrics across different platforms, as well as across 2D and 3D ASL MRI acquisitions as illustrated in Figure 2, and pseudo-ASL

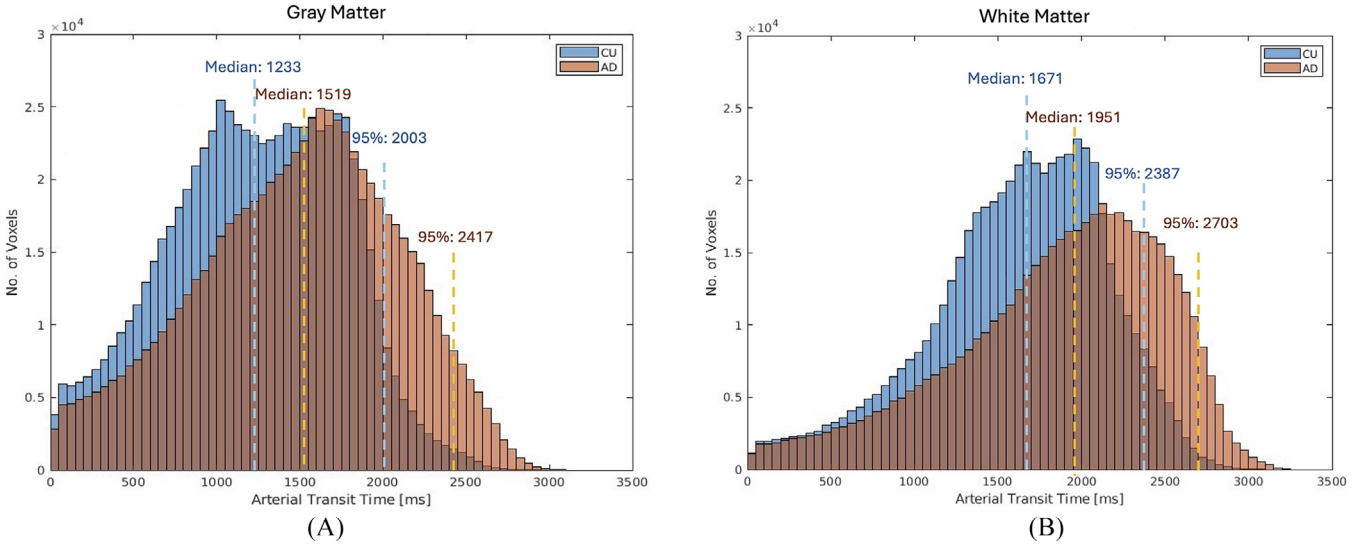

FIGURE 3 Distribution of ATT variability within GM and WM, assessed separately for AD and age- and sex-matched CU individuals ($n = 3$ in each group, 2 females and 1 male, mean age: 72 years), using a multi-PLD acquisition[49] at a 3T Siemens Skyra MR scanner. The plot illustrates the differences in ATT variability across tissue types and cognitive stages, emphasizing the challenges of using a single-PLD value in ASL imaging that generalizes to different tissue types and cohorts at different cognitive stages. AD, Alzheimer's disease; ASL, arterial spin labeling; ATT, arterial transit time; CU, cognitively unimpaired; GM, gray matter; PLD, post-labeling delay; WM, white matter.

(PASL) versus pseudo-continuous (pCASL) sequence types. These comparisons are crucial in understanding the potential sources of variability in ASL data and determining the optimal ASL acquisition techniques for future ADNI studies and clinical trials.

3 | ASL IN THE ADNI: THE PRESENT

In the past, single-PLD schemes dominated ASL imaging for most neuroimaging applications. This was fundamentally due to the limited SNR of ASL MRI, and the requirement to acquire multiple averages to achieve acceptable sensitivity. In general, a PLD corresponding to the time of the expected peak of the ASL inflow curve was chosen to maximize SNR. However, the timing of the ASL peak depends on the individual hemodynamics of the participant being scanned, and in situations in which the actual inflow curve is significantly shifted relative to the expected curve, large errors in CBF quantification will result. Figure 3 illustrates the distribution of ATT variability within gray matter (GM) and white matter (WM), assessed separately for AD and age- and sex-matched cognitively unimpaired (CU) individuals ($n = 3$ each group, 2 females/1 male, mean age: 72 years) using a multi-PLD technique[49] (data acquired in an independent study, separate from the ADNI cohort data collection). The results demonstrate significant differences across tissue types as well as cognitive stages. Therefore, while single-PLD protocols provide valuable insights, they have important limitations in quantifying CBF in regions with delayed ATT.[46–49] Furthermore, the recruitment strategy for ADNI 4, which places a significant emphasis on the inclusion of participants from underrepresented populations and recognizes the importance of including individuals with cerebrovascular disease to better understand the complex interplay between cerebrovascular disease and AD, underscores the need for a robust method for CBF measurement.

Recognizing the need for CBF measurements that are accurate and robust to physiological state (i.e., less affected by inter-subject variations in ATT), the ADNI 4 has transitioned to a multi-PLD acquisition scheme. This scheme involves acquisition of multiple ASL images with varying delay timings after the labeling of arterial blood, thereby allowing for more accurate modeling and quantification of CBF across different vascular territories. This method provides a more comprehensive view of cerebral perfusion and enables improved characterization of cerebrovascular pathologies that are commonly comorbid with AD. In addition to enhanced CBF quantification, the multi-PLD scheme also provides valuable data on ATT, which can offer further insights into the cerebrovascular changes associated with cognitive decline and AD.[50,51] By providing a more complete picture of cerebral perfusion dynamics, the multi-PLD scheme is poised to improve our understanding of the complex interplay between AD and cerebrovascular disease.

However, while multi-PLD ASL MRI provides improved accuracy and the ability to measure both CBF and ATT simultaneously, it can result in decreased SNR and increased motion sensitivity, due to the distribution of sampling over the ASL inflow curve and the range of contrasts associated with this. For elderly subjects and individuals with AD and vascular comorbidities, this may negatively impact CBF quantification, though the inclusion of a PLD longer than 2 seconds is likely to improve the detection of the perfusion signal in these subjects. In addition, it is also important to reiterate the limitations of single-PLD ASL MRI. Specifically, single-PLD ASL MRI can be problematic when the ATT deviates significantly from the expected value. For participants with much longer ATT, single-PLD ASL MRI can result in unusable data

due to the predominance of vascular artifacts and negligible perfusion signal. Conversely, setting a very long PLD to accommodate extended ATT can lead to a significant loss of SNR in subjects with "normal" ATT, thereby affecting the overall quality of the data. Therefore, acquiring data with several PLDs is likely to improve robustness and result in a larger proportion of usable ASL MRI data sets for ADNI.

4 | SETTING UP MULTI-PLD ASL: THE JOURNEY

The decision process for the multi-PLD ASL MRI protocol design in ADNI 4 was influenced by several key factors, in line with the initiative's goal of validating biomarkers across diverse clinical imaging sites and MRI vendors, including Siemens, GE, and Philips. Striving for a balance between robust data acquisition and practical considerations, the protocol was designed to fit within a 7-minute acquisition time, including all prep and "dead" time, and to be based on product sequences without requiring vendor work-in-progress (WIP) or independently developed sequences, to avoid additional burden on sites. The chosen protocol, involving either 3D pCASL or 3D PASL, is needed to enable reliable estimation of CBF and ATT, considering the number of PLDs, range of PLDs, number of repeats, and the availability of head coils across platforms. The ultimate goal was to ensure cross-platform consistency, enabling the translation of findings to clinical trials and enhancing the utility and impact of ADNI 4.

The protocol design for multi-PLD ASL MRI in the ADNI 4 study also had to navigate vendor-specific limitations, as obtaining multi-PLD in a single sequence is not feasible for some vendors. This led to the development of a quasi multi-PLD ASL MRI approach (see below). In addition, each vendor has its own restrictions on PLD selection. For example, while Siemens offers full flexibility in PLD value selection, GE's 3D pCASL sequence is limited to certain predefined PLD values, and Philips' 3D pCASL sequence only allows for a maximum PLD of 2500 ms. These vendor-specific restrictions posed significant challenges and were crucial factors in the final protocol design.

The quasi-multi-PLD acquisition scheme consists of collecting single-PLD data in separate series for several PLDs and concatenating them in the first step of the processing pipeline to effectively create a multi-PLD data set. To accurately capture the ATT across different vascular territories, PLDs from 1000 to 3000 ms are included. As a strategic decision, five unique PLD values are selected within this range to limit the total ASL MRI acquisition time to < 7 minutes, when possible. With five PLDs, researchers can adequately sample the transit time curve for a broad range of ATTs (1000 ∼ 3000 ms). This approach maintains a feasible scan duration, minimizing patient discomfort and facilitating the integration of this protocol into routine clinical practice. Accordingly, the quasi multi-PLD sequences are included in the ADNI 4 with protocol parameters summarized in Table 2. For a sample ADNI 3 participant who later continued in the ADNI 4 study, their ADNI 3 single-PLD 3D PASL and ADNI 4 multi-PLD 3D pCASL imaging data collected on a 3T Siemens scanner are shown in Figure 4. These images highlight the value of the multi-PLD approach in providing regionally accurate CBF estimates and the ability to estimate ATT.

5 | REVIEW OF THE ADNI ASL MRI PUBLICATIONS

The inclusion of ASL MRI by the ADNI MRI Core has contributed to our understanding of the pathophysiology and progression of AD. Using standardized protocols and harmonizing multimodal and multidisciplinary data have not only expanded our imaging biomarker portfolio but also augmented research with existing AD biomarkers and cognitive measures. We conducted an exhaustive search across Web of Science, Google Scholar, PubMed, and Scopus, using specific keywords such as "ADNI," "ASL," "arterial spin labeling," and "cerebral blood flow." In addition, we reviewed the reference lists of key articles to ensure no significant publications were omitted. To the best of our knowledge, studies using ADNI ASL MRI data are discussed in this section. Several studies emerged based on the ASL MRI data combined with multidisciplinary biomarker and clinical data from the ADNI participants, whose details are summarized in Table 3.

Since its incorporation into the ADNI in 2009, ASL MRI has been included in several studies to analyze CBF as a measure of brain function and potential biomarker for AD pathology. At first, studies showed that data from ASL MRI and structural MRI, obtained in the same scan session, could give the same caliber of information as previous studies conducted with PET and single photon emission computed tomography.[52] In 2013, Wang et al. reported the complementary information from structural MRI and ASL MRI data by tracking measures across CU to MCI individuals.[5] Meta-region of interest (ROI) (precuneus, bilateral parietal cortex, and bilateral temporal cortex) CBF measures were associated with diagnostic groups, with significant hypoperfusion observed in late MCI and AD compared to CU individuals.[5] Next, structural and CBF (multimodal) changes were analyzed more specifically in relation to AD biomarkers. With acquisitions from the ADNI GO and ADNI 2 cycles, multimodal MRI was used to classify brain amyloid positivity (amyloid+ or amyloid−) in early AD with high accuracy and sensitivity (83% and 87%, respectively).[3] The same approach was then applied to all diagnostic groups of AD, expanding across the breadth of the disease continuum. Results showed that amyloid pathology affected CBF across the AD spectrum, with lower regional CBF associated with higher amyloid load early on, and GM volume higher later in the disease (late MCI and AD dementia).[7] In 2016, Iturria-Medina et al. analyzed changes from a spatiotemporal lens using multifactorial data from amyloid PET, cerebrospinal fluid (CSF) and plasma proteins, ASL MRI, FDG PET, structural MRI, resting state functional MRI (fMRI) from individuals across the AD spectrum, specifically focusing on late-onset AD (LOAD). They reported that vascular dysfunction is an early event associated with LOAD, followed by amyloid pathology and the known amyloid/tau/neurodegeneration (ATN) cascade seen in AD.[9] This work laid the foundation for using multimodal imaging to connect structural and neural characteristics with known AD biomarkers and outcomes of disease progression.

Memory performance is an important clinical outcome measure of AD, particularly as a measure of success in clinical trials. Thus, linking memory performance with individual AD biomarker measures such as amyloid, tau, metabolism, and CBF allows researchers to gain

TABLE 2 Quasi Multi-PLD ASL MRI acquisition types used in ADNI 4 cycle.

	Siemens 3D PASL[b]	Siemens 3D pCASL	Philips 3D pCASL	GE 3D pCASL
Software versions	Prisma VE11C/VE11E Skyra VE11C Vida XA20	XA30 Vida XA50	Advanced 5.6	MR750: 29.0 8ch Basic, 29.1 8ch Basic, 29.1 32ch Nova Advanced Premier: 29.0 48ch Basic, 29.1 48ch Advanced
TR	4000 ms	XA30: 5533 ms XA50: 5110 ms	4850 ms	4533–4706 ms
TE	20.26 ms	XA30: 14.4 ms XA50: 16.6 ms	9 ms	12.556 ms
Field of view	240×240 mm^2	230×230 mm^2	240×240 mm^2	240×240 mm^2
Acquisition matrix	64×64	64×64	68×62	N/A
Reconstruction matrix	128×128	128×128	96×96	128×128
Spatial resolution	$1.875 \times 1.875 \times 4.5$ mm^3	$1.8 \times 1.8 \times 4.0$ mm^3	$2.5 \times 2.5 \times 4.5$ mm^3	$1.875 \times 1.875 \times 4.5$ mm^3
Bandwidth	2442 Hz/pix	XA30: 3396 Hz/pix XA50: 3444 Hz/pix	1898.9 Hz/pix	976.6 Hz/pix
Background suppression	Yes	Yes	Yes	Yes
Readout	EPI	GRASE	GRASE	Stack of spirals
Bolus duration	800 ms	1800 ms	1800 ms	1800 ms
TIs/PLDs	1000, 1500, 2000, 2510, 3000 ms	XA30: 1260, 1500, 2000, 2500, 3000 ms XA50: 1000, 1500, 2000, 2500, 3000 ms	1000, 1500, 1750, 2000, 2500 ms	1025, 1525, 2025, 2525, 3025 ms
M0	No	XA30: Yes, single M0 XA50: Yes, per PLD	Yes, with PLD = 2500 ms; 2 repeats	Yes, per PLD
Control-tag pairs available	Yes	Yes	Yes	No[a]
Number of repeats per PLD	2	1	1 for PLD = 1000 –2000 ms 2 for PLD = 2500 ms	1
Acquisition time	5:40-8:20 min	XA30: 5:26 min XA50: 5:40 min	8:15 min	7:17 min
Number of segments/arms	4	4	6	6
Number of points per arm	N/A	N/A	N/A	768

Abbreviations: ADNI, Alzheimer's Disease Neuroimaging Initiative; ASL, arterial spin labeling; MRI, magnetic resonance imaging; PASL, pseudo- arterial spin labeling; pCASL, pseudo-continuous arterial spin labeling; PLD, post-labeling delay; TE, echo time; TR, repetition time.

[a]Provided as vendor estimated perfusion-weighted tag—control difference images.

[b]As 3D pCASL becomes available as a product sequence in upgraded platforms, the sites will transition to 3D pCASL protocols. While this is not ideal from a longitudinal perspective, it maximizes the quality of ASL MRI data being generated and harmonization across vendors.

insight into the pathophysiological progression of AD. Both hypoperfusion and hyperperfusion have been associated with variable cognition across the clinical spectrum, depending on disease stage and brain ROI.[7,14,22,53] Bangen et al. reported that individuals with higher amyloid burden showed significant negative associations between higher CBF in the hippocampus, posterior cingulate, and precuneus and worse memory performance, whereas amyloid– individuals showed no significant associations between CBF and memory performance. It was suggested that higher CBF (e.g., hyperperfusion) associated with worse cognition may be a response to vascular dysregulation with increased CBF needed to compensate for memory.[10] Weigand et al. found that lower CBF levels in older CU adults were more strongly associated with tau pathology than with amyloid pathology, and this was evident in measured objective and subjective memory outcomes.[22] Interestingly, older CU individuals who do not carry the *APOE* ε4 allele have higher CBF and better memory performance than those who carry the ε4 allele.[54] In a longitudinal (3-year follow-up) study, individuals who converted to dementia were found to have lower CBF (e.g., hypoperfusion) in inferior temporal and parietal regions, and this was associated with faster rates of decline with everyday functioning.[13]

The connection between memory performance and CBF has also been studied in cognitively impaired individuals. In 2020, Thomas et al.

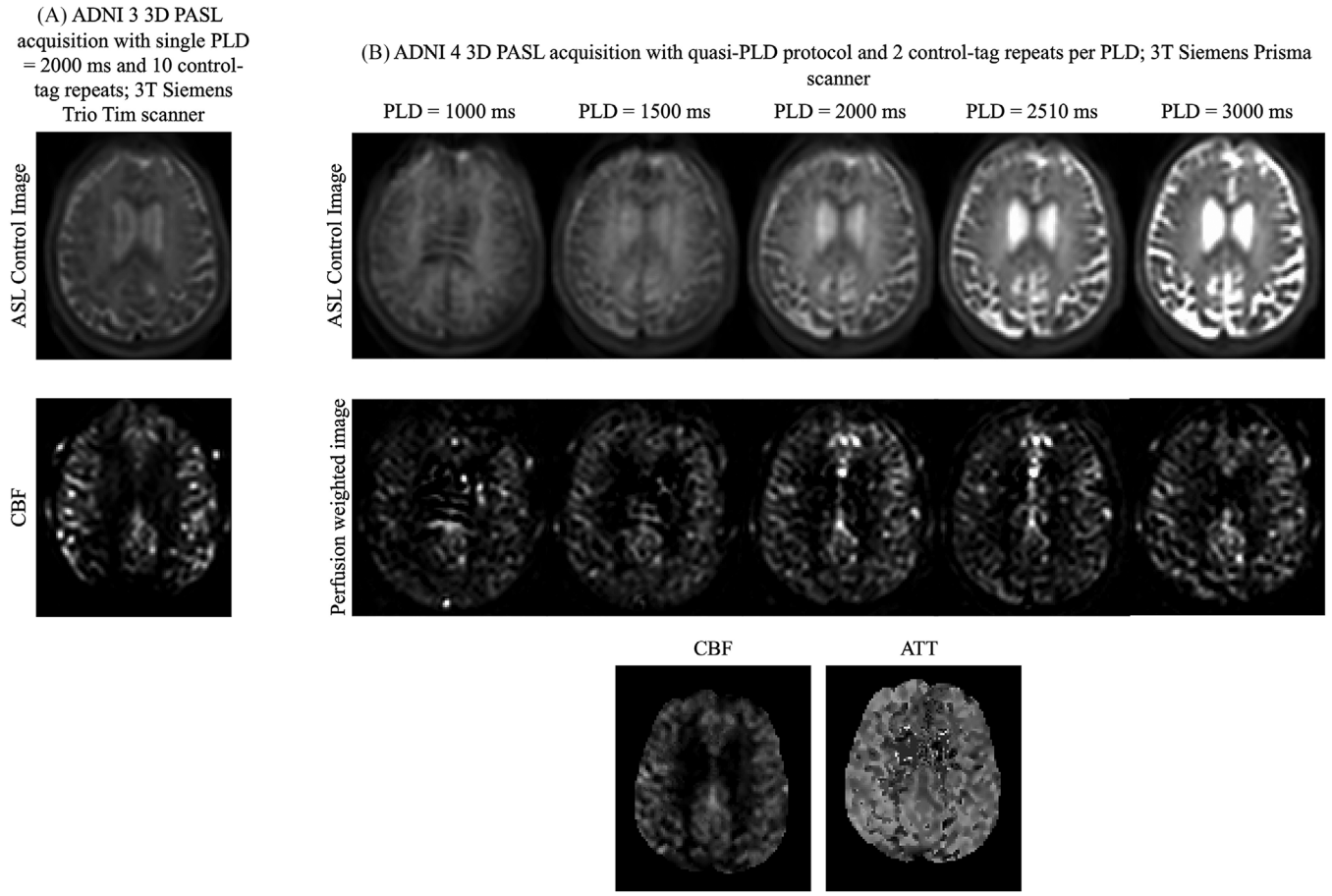

FIGURE 4 3D PASL acquisitions from a CU 73-year-old male subject illustrating the quality of improvement from single-PLD ADNI 3 protocol to multi-PLD ADNI 4 protocol. CBF is presented as mL/100 g/min. ATT is in seconds. ASL MRI data were acquired 1 year apart. ADNI, Alzheimer's Disease Neuroimaging Initiative; ASL, arterial spin labeling; ATT, arterial transit time; CBF, cerebral blood flow; CU, cognitively unimpaired; MRI, magnetic resonance imaging; PASL, pseudo-ASL; PLD, post-labeling delay.

reported that patterns of regional CBF are complex and vary across AD diagnostic groups.[14] Individuals with objectively defined subtle cognitive decline (early stage of AD) had hyperperfusion in hippocampal and inferior parietal regions compared to CU and MCI groups, and also in the inferior temporal region relative to MCI, while there were no perfusion differences in the frontal regions. This is in line with higher CBF being detected in earlier, prodromal stages of AD compared to individuals who have progressed further and have cognitive impairment, perhaps indicating a cognitive reserve or protective feature. CBF–tau associations were identified to be related to cognition, confirmed with PET, and reported to be driven in part by amyloid burden.[15] Further, modeling of entorhinal CBF, adjusted for AD biomarkers, demographic characteristics, and pulse pressure, showed that hypoperfusion predicts faster rates of memory issues, atrophy, and small vessel cerebrovascular disease,[11] suggesting that CBF may be a useful predictive AD biomarker. Holmqvist et al. examined within-person cognitive variability and found that amyloid burden is associated with hypoperfusion and cognitive function in older individuals and that individuals with AD biomarker positivity (amyloid+/phosphorylated tau+) had higher cognitive variability and lower CBF in entorhinal and hippocampal regions over a 12-month longitudinal analysis.[20,21] Higher cognitive reserve, estimated from a verbal intelligence quotient, was found to protect the brain from cognitive changes in MCI individuals, linking CBF with language fluency.[24]

Regional hypoperfusion is regularly identified in individuals who have amyloid and tau burden.[16,18,19,21,23,25] A recent retrospective analysis by Kapadia et al. analyzed perfusion in CU and MCI individuals from ADNI 2 and found that hypoperfusion is correlated with eventual tau deposition in the entorhinal cortex and that lower CBF in this region occurs before tau deposition.[25] A comprehensive study of perfusion using ASL MRI, amyloid PET, and tau PET showed that hypoperfusion is associated with pathologic tau in early Braak stages, independent of amyloid status, vascular biomarkers, and *APOE* genotype.[18] Significant correlations were found between lower CBF and structural measurements (cortical volume, surface area, and thickness) across AD diagnostic groups.[26] Using causal mediation analyses, Bilgel et al. reported that higher inferior temporal tau was associated with hypoperfusion, lower glucose metabolism, and lower regional volume independent of amyloid pathology.[19]

Genetic AD risk factors have been studied using ASL MRI. A single nucleotide polymorphism (SNP) of *ABCC9* known to be associated with hippocampal sclerosis was found to be associated with decreased

TABLE 3 Demographic characteristics and AD biomarker data availability for subjects with ASL data by ADNI study cycle and ASL type, as of April 2024.

	ADNIGO	ADNI2	ADNI3			
	Siemens 2D PASL	Siemens 2D PASL	Siemens2D PASL	Philips 2D PASL	Siemens 3D PASL	GE 3D pCASL
Age at baseline (years)	70 ± 6.3	73 ± 7.3	72 ± 7.8	74 ± 8.2	72 ± 8.3	74 ± 7.4
Sex (M/F)	29/13	197/176	58/90	85/78	209/247	112/103
Race (White/Black/Asian/Other or More than one)	40/1/0/1	344/17/5/8	88/21/4/6	139/3/1/1	324/55/21/8	185/13/4/4
Ethnicity (Hispanic or Latino/not Hispanic or Latino)	2/40	8/366	11/108	5/139	41/375	12/193
Years of education	16 ± 2.5	16 ± 2.7	16 ± 2.3	17 ± 2.4	16 ± 2.4	16 ± 2.5
Clinical diagnosis at baseline (CU/MCI/dementia)	3/21/1	55/76/26	79/31/8	62/68/10	242/140/28	111/67/26
APOE ε4 carriers	13	162	33	51	120	74
MMSE at baseline	28 ± 4.3	27 ± 3.3	28 ± 2.3	28 ± 2.4	27 ± 2.9	28 ± 2.9
CDR-SB at baseline	1.3 ± 1.7	1.5 ± 2.5	0.76 ± 1.6	1.3 ± 1.8	0.96 ± 1.7	1.4 ± 2.2
ADAS-Cog13 at baseline	10 ± 11	15 ± 11	12 ± 8.7	13 ± 8.9	13 ± 8.9	14 ± 10
Amyloid PET availability	40	347	106	129	374	189
Tau PET availability	0	37	101	116	341	181
CSF biomarker availability	34	292	56	93	195	105
Total number of scans	113	1555	276	392	837	523
Total number of subjects	47	385	148	163	456	215

Abbreviations: AD, Alzheimer's disease; ADAS-Cog13, Alzheimer's Disease Assessment Scale, 13-item cognitive subscale; ADNI, Alzheimer's Disease Neuroimaging Initiative; *APOE*, apolipoprotein E; ASL, arterial spin labeling; CDR-SB, Clinical Dementia Rating Sum of Boxes; CSF, cerebrospinal fluid; CU, cognitively unimpaired; MCI, mild cognitive impairment; MMSE, Mini-Mental State Examination; PASL, pseudo arterial spin labeling; PET, positron emission tomography; pCASL, pseudo-continuous arterial spin labeling.

CBF.[55] In 2019, Yao et al. explored how genes associated with AD risk correlated with regional CBF. They found that a specific variant of the gene *INPP5D*, involved in downregulation of inflammation, had higher perfusion in the left angular gyrus, which suggests a potential protective role from AD pathology.[56] Calculated AD genetic risk scores from genome-wide association studies in addition to mRNA transcript expression of risk genes near the AD risk loci were found to be correlated with decreasing CBF across the lifespan,[57] indicating that expression of AD risk genes can affect CBF. Edwards et al. found a significant interaction between pulse pressure and *APOE* ε4 dose on CBF; higher pulse pressure was found to be associated with hypoperfusion in ε4 homozygous individuals in the entorhinal cortex, hippocampus, and inferior parietal cortex.[28]

Results from ASL MRI perfusion have also been studied as a marker for delayed blood delivery,[58] blood pressure variability,[59] connecting blood glucose and word memory,[60] and linking plasma neurofilament light chain to regional CBF[61] among AD groups.

Significant strides have been made recently that contribute to improving ASL MRI processing and analysis, and many of these technical developments leveraged ADNI ASL MRI data in their methods development and validation. Using machine learning techniques, Bron et al. used CBF and GM volume to diagnostically classify early-stage dementia individuals who were suspected of having either AD or FTD. ASL was not found to have added value over atrophy markers.[62] Cselényi and Farde found that quasi-steady-state standardized uptake value ratio values of amyloid PET measurements were sensitive to changes in regional CBF, and this significant effect increased with disease progression,[8] advocating for amyloid pathology burden quantification approaches not sensitive to this effect. The algorithm SCORE (Structural Correlation-based Outlier REjection) was introduced to remove artifacts and clean outliers from 2D PASL data and showed improved CBF quantification.[63] Dolui et al. also reported that background suppressed (BS) 3D pCASL is more sensitive than PASL and 2D pCASL in regional CBF of MCI individuals.[64] Li et al. presented an improved method using prior-guided and slice-wise outlier rejection.[65] ASL-MRICloud was established as a remote tool for ASL MRI processing from all major vendors and acquisition types, and its veracity was tested on ASL MRI data from the ADNI.[66] Li et al. also proposed a sparse regression algorithm to infer integrated hyper-connectivity networks from blood oxygen–level dependent fMRI and ASL MRI using

functionally weighted least absolute shrinkage and selection operator (LASSO) for classification. This method outperformed what was being used at that time.[67] A VAE-GAN (Variational Auto-Encoder Generative Adversarial Network) model was introduced by Li et al. to synthesize ASL images.[68] Zhang et al. slightly improved sensitivity of ASL MRI by training deep learning models using data from healthy individuals and then transferring to pCASL data of older AD individuals.[69] Personalized brain models were introduced by Khan et al. that integrated multimodal neuroimaging and neurotransmitter receptor data. Results showed that mechanisms that affect CBF and GM atrophy contributed to most of the variability among individuals.[70] Camargo and Wang compared sensitivity and performance of ASL MRI among three commercial sequences (2D PASL, 3D BS PASL, and 3D BS pCASL) to distinguish among controls, MCI, and AD individuals. They found that 3D BS pCASL detected more widespread differences in CBF and revealed an interesting pattern in the orbito-frontal cortex related to change from normal to MCI to AD.[71] Li et al. found disruptions in the topological organization of CBF correlation networks that differed between the two diagnostic groups.[29] An automated and objective quality evaluation index (QEI) for ASL CBF maps was introduced by Dolui et al. to provide a metric for CBF map quality. This method was shown to work through common artifacts and was comparable to manual examination.[72] Finally, Shyna et al. recently proposed and validated a 2D convolutional neural network architecture to increase SNR and resolution while retaining edge information using ASL MRI from the ADNI.[73] While the ADNI ASL MRI data set can be used to help validate and test novel processing and analysis methods, it is of course possible to process the data using standard, generally available ASL MRI software tools (e.g., those listed in Fan et al.[74]); most studies involving ADNI ASL MRI data have indeed been analyzed in this way.

6 | OTHER MULTI-CENTER STUDIES USING ASL MRI

In parallel with ADNI, several other large multicenter neuroimaging studies have also incorporated ASL MRI into their neuroimaging protocols. Some of these, particularly those focusing on dementia and/or other neurodegenerative diseases, have chosen to align with the ADNI ASL MRI protocol, to facilitate comparison and possible merging of data sets. For example, the Dominantly Inherited Alzheimer's Network (DIAN) study[75] MRI protocol includes the ADNI 3 ASL MRI sequence, as does the Longitudinal Early-Onset Alzheimer's Disease Study (LEADS)[76] and Standardized Centralized Alzheimer's and Related Dementias Neuroimaging (SCAN). Other large studies have implemented ASL MRI using slightly different acquisition schemes, either with single PLD (e.g., the Genetic Frontotemporal Initiative [GENFI][77,78]) or multi-PLD protocols (e.g., UK Biobank,[79] the Human Connectome Project [HCP][80]). Different objectives and restrictions on study design mean that the choice of ASL MRI acquisition parameters varies among these different studies, and this should be taken into account when comparing their ASL MRI results.

7 | LIMITATIONS/CHALLENGES

The analysis of ADNI ASL MRI presents several technical challenges and limitations that impact the accuracy and consistency of CBF measurements. Some of these challenges could be addressed through a multifaceted approach, but some intrinsic limitations persist.

One of the primary technical limitations of ASL MRI is SNR. Relatively low spatial resolution (compared to the anatomical scans) is used to achieve acceptable SNR and precision in the output CBF maps. While isotropic resolution is possible, it is more typical to acquire ASL MRI with anisotropic voxels, with higher in-plane resolution and thicker slices. For 2D multi-slice acquisitions, this enables whole-brain coverage while keeping the between-slice variation of PLD within an acceptable range; for 3D acquisitions, thicker slices keep the number of segments (and therefore the overall acquisition time) to a reasonable value. For the ADNI cohort, we were careful to design the protocol to try to avoid long scans, for reasons of patient comfort and to avoid data corruption from motion artifacts.

7.1 | Biological and scanner variability

ASL MRI studies have been challenging to a large degree because SNR is low and biological variations are difficult to control. To reduce variability in ASL MRI data, the processing steps can include (1) co-registration of ASL MRI to the corresponding structural MRI data using a combination of linear and non-linear registration to account for global and local alignment; (2) intensity normalization concerning the corresponding ASL reference scan signal without background suppression and labeling (i.e., M0 image) to account for B1-field inhomogeneity and other instrumental variations, and to enable accurate CBF quantification; (3) intensity calibration to the mean value of perfusion from a reference brain region to account for global variations in CBF from scan to scan;[81,82] and (4) correction for partial volume effects (PVE) to account for underlying structural variations in brain atrophy and in GM/WM voxel composition using information from the probabilistic tissue segmentation maps of structural MRI co-registered to ASL MRI.

7.2 | Lack of M0 images and calibration challenges across multiple PLDs

One of the primary challenges with certain acquisition protocols (cf Tables 1–2) is the absence of M0 images, used for perfusion calibration to achieve quantitative CBF measures in mL/g/min units. To circumvent this, background-suppressed control images are used as a surrogate for M0 by scaling up the control images by the background suppression factor. This method has proven effective for single-PLD ASL with high SNR. However, its efficacy for multi-PLD ASL data sets remains to be validated. The variability in CSF signal across different PLDs, due to non-ideal background suppression, means that it may be preferable to use a subset of the control images for M0 approximation.

Furthermore, the heterogeneity in sequence timing—some sequences extend the repetition time (TR) with increasing PLD—leads to an "effective M0" that may vary across PLDs. This introduces extra complications for CBF quantification, which have yet to be fully addressed.

7.3 | Vascular contributions to the ASL signal

The labeling and image acquisition processes in ASL MRI occur on a time scale of a few seconds, which is similar to the time taken for blood to travel from the labeling plane to the capillary bed of the brain. Consequently, it is expected that the ASL MRI signal will contain a mixed contribution from intra- and extravascular water. ASL MRI quantification models typically assume that the labeled bolus is fully delivered to the tissue, and in situations in which this is not true (e.g., in patients with unusually long ATT), strong vascular artifacts (known as "arterial transit artifacts," or ATAs[83,84]) caused by signal in the large arteries and arterioles will be seen. For single PLD acquisitions, this is especially problematic, as the characteristic focal hyperintense signal will cause local overestimation of CBF. Vascular crusher gradients can be used to eliminate intravascular signal, but errors in CBF quantification still result, due to incomplete delivery of the bolus. Multi-PLD ASL MRI can help address this issue by sampling the inflow curve more completely, thereby enabling the use of more complex and realistic biophysical models that include an intravascular compartment.[85] Separation of the signal into "macrovascular" and "perfusion" components also opens up the possibility of analyzing these signals independently, potentially providing complementary insight into the different blood flow–related aspects of neurodegenerative disease.

7.4 | Measuring WM and GM perfusion

The optimal ASL MRI sensitive to WM perfusion often requires a long measurement time, extended labeling duration, and a long PLD. However, we recognize that a single protocol cannot be perfectly optimized for both GM and WM perfusion. Multi-PLD ASL MRI represents a balanced approach to measuring both GM and WM perfusion. Multi-PLD ASL MRI sequences include PLDs much longer than those typically used for single-PLD scans, which can help with WM CBF estimation and capturing perfusion signals in regions with delayed ATT. While the SNR may be decreased, the extended PLDs provide valuable data for assessing WM perfusion, crucial for understanding the pathophysiology of AD and its associated cerebrovascular components. This balanced approach ensures comprehensive perfusion measurements across both GM and WM, addressing the limitations of single-PLD ASL MRI protocols.

7.5 | Vendor-specific metadata inconsistencies

Diverse MRI vendors often supply insufficient or inconsistent metadata in Digital Imaging and Communications in Medicine headers. Comprehensive and precise metadata are crucial for CBF computation, and most quantification software relies on this data for automatic parameter entry during ASL MRI processing. Missing information, such as bolus/labeling duration, echo spacing, dwell time (for EPI distortion correction), and slice-to-slice delay time (for 2D EPI) significantly hampers straightforward data processing and quantification, which is essential in large cohort studies such as the ADNI.

7.6 | Harmonization across ASL MRI types

Although both PASL and pCASL methods label blood water by inversion of its magnetization, the differences in how this is achieved result in significant variations in the contrast of the subsequent perfusion-weighted images. Due to the relatively short bolus duration and inflow time (TI2-TI1), which is required to minimize T1 relaxation of the labeled blood and retain acceptable SNR, PASL tends to be more prone to ATAs and unwanted intravascular signal than pCASL, especially in elderly populations. This can lead to larger errors in CBF quantification and misinterpretation of results, for example, prolonged transit times often accompany low CBF in the parenchyma and high CBF in or near feeding arteries. Due to the continuous inversion process, pCASL can use longer, more optimal labeling durations, and a wider range of PLDs, which help to avoid the appearance of vascular artifacts or enable better characterization and modeling of them, as well as improve the SNR of the perfusion signal. For these reasons, ADNI 4 has shifted toward using multi-PLD pCASL; however, when analyzing ASL data from previous cycles of ADNI, and combining data that have been acquired with different ASL methods, it is important to keep these intrinsic differences in mind. The differences could also be sensitive to the biological factors affecting the blood flow dynamics, such as the impact of arterial stiffness on blood velocity, which can differ with pathology and age.

7.7 | Motion sensitivity for 3D sequences

3D sequences are now most commonly used for ASL, due to their intrinsic SNR benefits and their straightforward compatibility with background suppression. However, complete 3D data sets cannot be acquired within a single excitation (or shot) while still achieving whole-brain coverage and an acceptable image point spread function, so data collection for individual ASL MRI volumes must be spread out over multiple TR periods. This inevitably leads to some motion sensitivity, which can cause image artifacts and compromise the reliability of the resulting quantitative CBF and ATT maps. Recent advances in rapid imaging technologies, such as compressed sensing and deep learning–based reconstructions, offer the possibility of single-shot acquisitions in the future. For now, however, it is important to implement rigorous image quality control procedures as part of the post-processing pipeline, and to reject sufficiently corrupt data from the analysis, ideally using either visual quality control assessment approaches or objective and automated approaches.[86]

7.8 | ASL MRI in the ADNI: the future

The advancement of multi-PLD ASL MRI techniques holds promise for significantly enhancing our understanding of AD progression. Sampling of multiple points along the dynamic ASL inflow curve using multi-PLD enables characterization of ATT, which is known to be prolonged in cerebrovascular disease and with age,[86–89] therefore making it particularly suited to investigating early AD stages and associated cerebrovascular pathology. Modeling the dynamic changes in CBF and blood transit through the brain can reveal early hemodynamic markers of AD before significant atrophy or cognitive decline occurs. Identifying these markers early could enable timely therapeutic interventions to slow disease progression. As AD and cerebrovascular disease share several pathophysiological features, complicating their prognosis and treatment, detailed characterization of ATT in conjunction with CBF could help distinguish vascular contributions to cognitive impairment and dementia from those due to primary neurodegenerative processes.[89,90]

Additionally, multi-PLD ASL MRI can deepen our understanding of AD pathophysiology by providing insights into cerebral hemodynamics. By providing a window into cerebral hemodynamics, we can study the relationship between CBF alterations and other biomarkers of AD, such as amyloid deposition and tau tangles.[9,91] A multimodality approach could elucidate the sequence of pathological events leading to AD and the role of vascular dysfunction in this cascade.[9]

Furthermore, multi-PLD ASL MRI can serve as a valuable tool for monitoring the efficacy of therapeutic interventions. Changes in ATT and CBF after treatment can indicate the therapy's impact on brain health and function.[92,93] This objective measure could accelerate the evaluation of new drugs or treatment protocols, potentially speeding up the development of effective AD therapies.

Finally, continuous advancements in ASL MRI methodology, including the use of higher magnetic field strengths and more sophisticated post-processing techniques, will further refine CBF quantification. The integration of multi-PLD ASL MRI with other imaging modalities, such as PET (amyloid and tau) and structural MRI, promises to provide a more holistic picture of the AD brain. Improved hardware, such as stronger gradients and better coil technology, coupled with innovative software algorithms, will enhance SNR and spatial resolution, potentially making it possible to detect even earlier CBF changes.

8 | SUMMARY

The use of ASL MRI in the ADNI has evolved over the years, driven by advances in technology and the need for more detailed and reliable measurements of cerebral perfusion. Despite the challenges encountered, the incorporation and expansion of ASL MRI in the ADNI has proven invaluable in enhancing our understanding of AD and its associated changes in CBF. In designing the ADNI ASL study, we have incorporated data and findings from several independent studies. These prior studies form the foundation and motivation for our approach, ensuring that our study is built on well-established scientific principles and prior evidence.

The transition to multi-PLD ASL MRI reaffirms the ADNI's commitment to driving innovation in AD research. Through more precise and comprehensive CBF measurements, this technique holds promise in advancing our understanding of AD and its common comorbid condition, cerebrovascular disease.

ACKNOWLEDGMENTS

Data collection and sharing for this project was funded by the Alzheimer's Disease Neuroimaging Initiative (ADNI; National Institutes of Health Grant U01 AG024904) and DOD ADNI (Department of Defense award number W81XWH-12-2-0012). ADNI is funded by the National Institute on Aging, the National Institute of Biomedical Imaging and Bioengineering, and through generous contributions from the following: AbbVie; Alzheimer's Association; Alzheimer's Drug Discovery Foundation; Araclon Biotech; BioClinica, Inc.; Biogen; Bristol-Myers Squibb Company; CereSpir, Inc.; Cogstate; Eisai Korea Inc.; Elan Pharmaceuticals, Inc.; Eli Lilly and Company; EuroImmun; F. Hoffmann-La Roche Ltd and its affiliated company Genentech, Inc.; Fujirebio; GE Healthcare; IXICO Ltd.; Janssen Alzheimer Immunotherapy Research & Development, LLC; Johnson & Johnson Pharmaceutical Research & Development LLC; Lumosity; Lundbeck; Merck & Co., Inc.; Meso Scale Diagnostics, LLC; NeuroRx Research; Neurotrack Technologies; Novartis Pharmaceuticals Corporation; Pfizer Inc.; Piramal Imaging; Servier; Takeda Pharmaceutical Company; and Transition Therapeutics. The Canadian Institutes of Health Research is providing funds to support ADNI clinical sites in Canada. Private sector contributions are facilitated by the Foundation for the National Institutes of Health (www.fnih.org). The grantee organization is the Northern California Institute for Research and Education, and the study is coordinated by the Alzheimer's Therapeutic Research Institute at the University of Southern California. ADNI data are disseminated by the Laboratory for Neuro Imaging at the University of Southern California.

CONFLICTS OF INTEREST STATEMENT

P.T., E.P., Y.J., D.L.T., and D.T. have no conflicts of interest. D.L.T. is supported by the UCLH NIHR Biomedical Research Centre. Author disclosures are available in the supporting information.

CONSENT STATEMENT

ADNI study was approved by each ADNI study site's respective institutional review board and informed written consent was obtained from all participants.

ORCID

Pamela Thropp https://orcid.org/0009-0006-5371-8667
Duygu Tosun https://orcid.org/0000-0001-8644-7724

REFERENCES

1. Dai W, Lopez OL, Carmichael OT, Becker JT, Kuller LH, Gach HM. Mild cognitive impairment and Alzheimer disease: patterns of altered cerebral blood flow at MR imaging. *Radiology*. 2009;250:856-866.

2. Tosun D, Mojabi P, Weiner MW, Schuff N. Joint analysis of structural and perfusion MRI for cognitive assessment and classification of Alzheimer's disease and normal aging. *Neuroimage*. 2010;52:186-197.
3. Tosun D, Joshi S, Weiner MW; the Alzheimer's Disease Neuroimaging Initiative. Multimodal MRI-based imputation of the Aβ+ in early mild cognitive impairment. *Ann Clin Transl Neurol*. 2014;1:160-170.
4. Binnewijzend MA, Kuijer JP, Benedictus MR, et al. Cerebral blood flow measured with 3D pseudocontinuous arterial spin-labeling MR imaging in Alzheimer disease and mild cognitive impairment: a marker for disease severity. *Radiology*. 2013;267:221-230.
5. Wang Z, Das SR, Xie SX; the Alzheimer's Disease Neuroimaging Initiative, et al. Arterial spin labeled MRI in prodromal Alzheimer's disease: a multi-site study. *NeuroImage Clin*. 2013;2:630-636.
6. Mak HK, Qian W, Ng KS, et al. Combination of MRI hippocampal volumetry and arterial spin labeling MR perfusion at 3-Tesla improves the efficacy in discriminating Alzheimer's disease from cognitively normal elderly adults. *J Alzheimers Dis*. 2014;41:749-758.
7. Mattsson N, Tosun D, Insel PS, et al. Association of brain amyloid-β with cerebral perfusion and structure in Alzheimer's disease and mild cognitive impairment. *Brain*. 2014;137:1550-1561.
8. Cselényi Z, Farde L. Quantification of blood flow-dependent component in estimates of beta-amyloid load obtained using quasi-steady-state standardized uptake value ratio. *J Cereb Blood Flow Metab*. 2015;35:1485-1493.
9. Iturria-Medina Y, Sotero RC, Toussaint PJ, Mateos-Pérez JM, Evans AC; the Alzheimer's Disease Neuroimaging Initiative. Early role of vascular dysregulation on late-onset Alzheimer's disease based on multifactorial data-driven analysis. *Nat Commun*. 2016;7:11934.
10. Bangen KJ, Clark AL, Edmonds EC, et al. Cerebral blood flow and amyloid-β interact to affect memory performance in cognitively normal older adults. *Front Aging Neurosci*. 2017;9:181.
11. Bangen KJ, Thomas KR, Sanchez DL, et al. Entorhinal perfusion predicts future memory decline, neurodegeneration, and white matter hyperintensity progression in older adults. *J Alzheimers Dis*. 2021;81:1711-2175.
12. Dougherty RJ, Boots EA, Lindheimer JB, et al. Fitness, independent of physical activity is associated with cerebral blood flow in adults at risk for Alzheimer's disease. *Brain Imaging Behav*. 2020;14:1154-1163.
13. Sanchez DL, Thomas KR, Edmonds EC, Bondi MW, Bangen KJ; the Alzheimer's Disease Neuroimaging Initiative. Regional hypoperfusion predicts decline in everyday functioning at three-year follow-up in older adults without dementia. *J Alzheimers Dis*. 2020;77:1291-1304.
14. Thomas KR, Osuna JR, Weigand AJ, et al. Regional hyperperfusion in older adults with objectively-defined subtle cognitive decline. *J Cereb Blood Flow Metab*. 2021;41:1001-1012.
15. Albrecht D, Isenberg AL, Stradford J, et al. Associations between vascular function and tau PET are associated with global cognition and amyloid. *J Neurosci*. 2020;40:8573-8586.
16. Camargo A, Wang Z; the Alzheimer's Disease Neuroimaging Initiative. Longitudinal cerebral blood flow changes in normal aging and the Alzheimer's disease continuum identified by arterial spin labeling MRI. *J Alzheimers Dis*. 2021;81:1727-1735.
17. Duan W, Zhou GD, Balachandrasekaran A, et al. Cerebral blood flow predicts conversion of mild cognitive impairment into Alzheimer's disease and cognitive decline: an arterial spin labeling follow-up study. *J Alzheimers Dis*. 2021;82:293-3205.
18. Rubinski A, Tosun D, Franzmeier N, et al. Lower cerebral perfusion is associated with tau-PET in the entorhinal cortex across the Alzheimer's continuum. *Neurobiol Aging*. 2021;102:111-118.
19. Bilgel M, Wong DF, Moghekar AR, Ferrucci L, Resnick SM; the Alzheimer's Disease Neuroimaging Initiative. Causal links among amyloid, tau, and neurodegeneration. *Brain Commun*. 2022;4:fcac193.
20. Holmqvist SL, Thomas KR, Brenner EK, et al. Longitudinal intraindividual cognitive variability is associated with reduction in regional cerebral blood flow among Alzheimer's disease biomarker-positive older adults. *Front Aging Neurosci*. 2022;14:859873.
21. Holmqvist SL, Thomas KR, Edmonds EC; the Alzheimer's Disease Neuroimaging Initiative, et al. Cognitive dispersion is elevated in amyloid-positive older adults and associated with regional hypoperfusion. *J Int Neuropsychol Soc*. 2023;29:621-631.
22. Weigand AJ, Hamlin AM, Breton J, Clark AL. Cerebral blood flow, tau imaging, and memory associations in cognitively unimpaired older adults. *Cereb Circ Cogn Behav*. 2022;3:100153.
23. Ahmadi K, Pereira JB, Berron D, et al. Gray matter hypoperfusion is a late pathological event in the course of Alzheimer's disease. *J Cereb Blood Flow Metab*. 2023;43:565-580.
24. Brenner EK, Thomas KR, Weigand AJ, et al. Cognitive reserve moderates the association between cerebral blood flow and language performance in older adults with mild cognitive impairment. *Neurobiol Aging*. 2023;125:83-89.
25. Kapadia A, Billimoria K, Desai P, et al. Hypoperfusion precedes tau deposition in the entorhinal cortex: a retrospective evaluation of ADNI-2 data. *J Clin Neurol*. 2023;19:131-137.
26. Nabizadeh F, Balabandian M, Rostami MR, Mehrabi S, Sedighi M; the Alzheimer's Disease Neuroimaging Initiative. Regional cerebral blood flow and brain atrophy in mild cognitive impairment and Alzheimer's disease. *Neurol Lett*. 2023;2:16-24.
27. Swinford CG, Risacher SL, Vosmeier A, et al. Amyloid and tau pathology are associated with cerebral blood flow in a mixed sample of nondemented older adults with and without vascular risk factors for Alzheimer's disease. *Neurobiol Aging*. 2023;130:103-113.
28. Edwards L, Thomas KR, Weigand AJ, et al. Pulse pressure and APOE ε4 dose interact to affect cerebral blood flow in older adults without dementia. *Cereb Circ Cogn Behav*. 2024;6:100206.
29. Li M, Zhu T, Kang Y, Qi S. A 3D pseudo-continuous arterial spin labeling study of altered cerebral blood flow correlation networks in mild cognitive impairment and Alzheimer's disease. *Front Aging Neurosci*. 2024;16:1345251.
30. Bryant AG, Manhard MK, Salat DH, et al. Heterogeneity of tau deposition and microvascular involvement in MCI and AD. *Curr Alzheimer Res*. 2021;18:711-720.
31. Jack CR Jr, Andrews JS, Beach TG, et al. Revised criteria for diagnosis and staging of Alzheimer's disease: Alzheimer's Association Workgroup. *Alzheimers Dement*. 2024;20:5143-5169.
32. Detre JA, Leigh JS, Williams DS, Koretsky AP. Perfusion imaging. *Magn Reson Med*. 1992;23:37-45.
33. Roberts DA, Detre JA, Bolinger L, Insko EK, Leigh JS Jr. Quantitative magnetic resonance imaging of human brain perfusion at 1.5 T using steady-state inversion of arterial water. *Proc Natl Acad Sci USA*. 1994;91:33-37.
34. Alsop DC, Detre JA, Golay X, et al. Recommended implementation of arterial spin-labeled perfusion MRI for clinical applications: a consensus of the ISMRM perfusion study group and the European consortium for ASL in dementia. *Magn Reson Med*. 2015;73:102-116.
35. Buxton RB. Quantifying CBF with arterial spin labeling. *J Magn Reson Imaging*. 2005;22:723-726.
36. Detre JA, Wang J, Wang Z, Rao H. Arterial spin-labeled perfusion MRI in basic and clinical neuroscience. *Curr Opin Neurol*. 2009;22:348-355.
37. Detre JA, Rao H, Wang DJ, Chen YF, Wang Z. Applications of arterial spin labeled MRI in the brain. *J Magn Reson Imaging*. 2012;35:1026-1037.
38. Wong EC. An introduction to ASL labeling techniques. *J Magn Reson Imaging*. 2014;40:1-10.
39. Chen Y, Wolk DA, Reddin JS, et al. Voxel-level comparison of arterial spin-labeled perfusion MRI and FDG-PET in Alzheimer disease. *Neurology*. 2011;77:1977-1985.
40. Musiek ES, Chen Y, Korczykowski M, et al. Direct comparison of fluorodeoxyglucose positron emission tomography and arterial spin

labeling magnetic resonance imaging in Alzheimer's disease. *Alzheimers Dement*. 2012;8:51-59.
41. Johnson NA, Jahng GH, Weiner MW, et al. Pattern of cerebral hypoperfusion in Alzheimer disease and mild cognitive impairment measured with arterial spin-labeling MR imaging: initial experience. *Radiology*. 2005;234:851-859.
42. Du AT, Jahng GH, Hayasaka S, et al. Hypoperfusion in frontotemporal dementia and Alzheimer disease by arterial spin labeling MRI. *Neurology*. 2006;67:1215-1220.
43. Hayasaka S, Du AT, Duarte A, et al. A non-parametric approach for co-analysis of multi-modal brain imaging data: application to Alzheimer's disease. *Neuroimage*. 2006;30:768-779.
44. Wang Y, Saykin AJ, Pfeuffer J, et al. Regional reproducibility of pulsed arterial spin labeling perfusion imaging at 3T. *Neuroimage*. 2011;54:1188-1195.
45. MacIntosh BJ, Swardfager W, Robertson AD, et al. Regional cerebral arterial transit time hemodynamics correlate with vascular risk factors and cognitive function in men with coronary artery disease. *AJNR Am J Neuroradiol*. 2015;36:295-301.
46. Woods JG, Achten E, Asllani I, et al. Recommendations for quantitative cerebral perfusion MRI using multi-timepoint arterial spin labeling: acquisition, quantification, and clinical applications. *Magn Reson Med*. 2024;92:469-495.
47. Campbell AM, Beaulieu C. Pulsed arterial spin labeling parameter optimization for an elderly population. *J Magn Reson Imaging*. 2006;23:398-403.
48. Mutsaerts HJ, van Osch MJ, Zelaya FO, et al. Multi-vendor reliability of arterial spin labeling perfusion MRI using a near-identical sequence: implications for multi-center studies. *Neuroimage*. 2015;113:143-152.
49. Johnston ME, Lu K, Maldjian JA, Jung Y. Multi-TI arterial spin labeling MRI with variable TR and bolus duration for cerebral blood flow and arterial transit time mapping. *IEEE Trans Med Imaging*. 2015;34:1392-3402.
50. Mak HK, Chan Q, Zhang Z, et al. Quantitative assessment of cerebral hemodynamic parameters by QUASAR arterial spin labeling in Alzheimer's disease and cognitively normal Elderly adults at 3-tesla. *J Alzheimers Dis*. 2012;31:33-44.
51. van der Thiel M, Rodriguez C, Van De Ville D, Giannakopoulos P, Haller S. Regional cerebral perfusion and cerebrovascular reactivity in elderly controls with subtle cognitive deficits. *Front Aging Neurosci*. 2019;11:19.
52. Tosun D, Schuff N, Jagust W, Weiner MW. Discriminative Power of Arterial Spin Labeling Magnetic Resonance Imaging and ^{18}F-Fluorodeoxyglucose Positron Emission Tomography Changes for Amyloid-β-Positive Subjects in the Alzheimer's Disease Continuum. *Neurodegenerative Diseases*. 2015;16(1–2):87-94. Portico. doi:10.1159/000439257
53. Yew B, Nation DA; the Alzheimer's Disease Neuroimaging Initiative. Cerebrovascular resistance: effects on cognitive decline, cortical atrophy, and progression to dementia. *Brain*. 2017;140:1987-2001.
54. Wang J, Peng G, Liu P, Tan X, Luo B; the Alzheimer's Disease Neuroimaging Initiative. Regulating effect of CBF on memory in cognitively normal older adults with different ApoE genotype: the Alzheimer's Disease Neuroimaging Initiative (ADNI). *Cogn Neurodyn*. 2019;13:513-518.
55. Ighodaro ET, Abner EL, Fardo DW, et al. Risk factors and global cognitive status related to brain arteriolosclerosis in elderly individuals. *J Cereb Blood Flow Metab*. 2017;37:201-216.
56. Yao X, Risacher SL, Nho K; the Alzheimer's Disease Neuroimaging Initiative, et al. Targeted genetic analysis of cerebral blood flow imaging phenotypes implicates the INPP5D gene. *Neurobiol Aging*. 2019;81:213-221.
57. Chandler H, Wise R, Linden D; the Alzheimer's Disease Neuroimaging Initiative, et al. Alzheimer's genetic risk effects on cerebral blood flow across the lifespan are proximal to gene expression. *Neurobiol Aging*. 2022;120:1-9.
58. Shirzadi Z, Stefanovic B, Mutsaerts H, Masellis M, MacIntosh BJ; the Alzheimer's Disease Neuroimaging Initiative. Classifying cognitive impairment based on the spatial heterogeneity of cerebral blood flow images. *J Magn Reson Imaging*. 2019;50:858-867.
59. Sible IJ, Yew B, Dutt S; the Alzheimer's Disease Neuroimaging Initiative, et al. Visit-to-visit blood pressure variability and regional cerebral perfusion decline in older adults. *Neurobiol Aging*. 2021;105:57-63.
60. Thomas KR, Weigand AJ, Cota IH; the Alzheimer's Disease Neuroimaging Initiative, et al. Intrusion errors moderate the relationship between blood glucose and regional cerebral blood flow in cognitively unimpaired older adults. *Brain Imaging Behav*. 2022;16:219-227.
61. Nabizadeh F, Ward RT, Balabandian M, Kankam SB, Pourhamzeh M. Plasma neurofilament light chain associated with impaired regional cerebral blood flow in healthy individuals. *Curr J Neurol*. 2023;22:221-230.
62. Bron EE, Steketee RM, Houston GC, et al. Diagnostic classification of arterial spin labeling and structural MRI in presenile early stage dementia. *Hum Brain Mapp*. 2014;35:4916-4931.
63. Dolui S, Wang Z, Shinohara RT, Wolk DA, Detre JA; the Alzheimer's Disease Neuroimaging Initiative. Structural Correlation-based Outlier Rejection (SCORE) algorithm for arterial spin labeling time series. *J Magn Reson Imaging*. 2017;45:1786-1797.
64. Dolui S, Vidorreta M, Wang Z, et al. Comparison of PASL, PCASL, and background-suppressed 3D PCASL in mild cognitive impairment. *Hum Brain Mapp*. 2017;38:5260-5273.
65. Li Y, Dolui S, Xie DF, Wang Z; the Alzheimer's Disease Neuroimaging Initiative. Priors-guided slice-wise adaptive outlier cleaning for arterial spin labeling perfusion MRI. *J Neurosci Methods*. 2018;307:248-253.
66. Li Y, Liu P, Li Y, et al. ASL-MRICloud: an online tool for the processing of ASL MRI data. *NMR Biomed*. 2019;32:e4051.
67. Li Y, Liu J, Gao X, et al. Multimodal hyper-connectivity of functional networks using functionally-weighted LASSO for MCI classification. *Med Image Anal*. 2019;52:80-96.
68. Li F, Huang W, Luo M, Zhang P, Zha Y. A new VAE-GAN model to synthesize arterial spin labeling images from structural MRI. *Displays*. 2021;70:102079.
69. Zhang L, Xie D, Li Y, et al. Improving sensitivity of arterial spin labeling perfusion MRI in Alzheimer's disease using transfer learning of deep learning-based ASL denoising. *J Magn Reson Imaging*. 2022;55:1710-1722.
70. Khan AF, Adewale Q, Baumeister TR, et al. Personalized brain models identify neurotransmitter receptor changes in Alzheimer's disease. *Brain*. 2022;145:1785-1804.
71. Camargo A, Wang Z; the Alzheimer's Disease Neuroimaging Initiative. Hypo- and hyper-perfusion in MCI and AD identified by different ASL MRI sequences. *Brain Imaging Behav*. 2023;17:306-319.
72. Dolui S, Wang Z, Wolf RL, et al. Alzheimer's disease neuroimaging initiative. Automated quality evaluation index for arterial spin labeling derived cerebral blood flow maps. *J Magn Reson Imaging*. 2024. Epub ahead of print. doi:10.1002/jmri.29308
73. Shyna A, Ushadevi AC, Ansamma J, Kesavadas C, Bejoy T, Anagha TJ. A mixed loss joint approach-based deep learning strategy to enhance SNR and resolution of arterial spin labelling MRI. *Int J Biomed Eng Technol*. 2024;44:324-347.
74. Fan H, Mutsaerts HJMM, Anazodo U, et al. ISMRM Open Science Initiative for Perfusion Imaging (OSIPI): ASL pipeline inventory. *Magn Reson Med*. 2024;91:1787-1802.
75. McKay NS, Gordon BA, Hornbeck RC; Dominantly Inherited Alzheimer Network, et al. Positron emission tomography and magnetic resonance imaging methods and datasets within the Dominantly Inherited Alzheimer Network (DIAN). *Nat Neurosci*. 2023;26:1449-1460.

76. Apostolova LG, Aisen P, Eloyan A; LEADS Consortium, et al. The Longitudinal Early-onset Alzheimer's Disease Study (LEADS): framework and methodology. *Alzheimers Dement*. 2021;17:2043-2055.
77. Mutsaerts H, Petr J, Thomas DL; GENFI investigators, et al. Comparison of arterial spin labeling registration strategies in the multi-center GENetic frontotemporal dementia initiative (GENFI). *J Magn Reson Imaging*. 2018;47:131-140.
78. Pasternak M, Mirza SS, Luciw N; GENetic Frontotemporal dementia Initiative (GENFI), et al. Longitudinal cerebral perfusion in presymptomatic genetic frontotemporal dementia: GENFI results. *Alzheimers Dement*. 2024;20:3525-3542.
79. Griffanti L, Raman B, Alfaro-Almagro F, et al. Adapting the UK Biobank brain imaging protocol and analysis pipeline for the C-MORE multi-organ study of COVID-19 survivors. *Front Neurol*. 2021;12:753284.
80. Juttukonda MR, Li B, Almaktoum R, et al. Characterizing cerebral hemodynamics across the adult lifespan with arterial spin labeling MRI data from the Human Connectome Project-Aging. *Neuroimage*. 2021;230:117807.
81. Aslan S, Lu H. On the sensitivity of ASL MRI in detecting regional differences in cerebral blood flow. *Magn Reson Imaging*. 2010;28:928-935.
82. Lacalle-Aurioles M, Alemán-Gómez Y, Guzmán-De-Villoria JA, et al. Is the cerebellum the optimal reference region for intensity normalization of perfusion MR studies in early Alzheimer's disease?. *PLoS One*. 2013;8:e81548.
83. Amukotuwa SA, Yu C, Zaharchuk G. 3D Pseudocontinuous arterial spin labeling in routine clinical practice: a review of clinically significant artifacts. *J Magn Reson Imaging*. 2016;43:11-27.
84. Lindner T, Bolar DS, Achten E, et al. Current state and guidance on arterial spin labeling perfusion MRI in clinical neuroimaging. *Magn Reson Med*. 2023;89:2024-2047.
85. Chappell MA, MacIntosh BJ, Donahue MJ, Günther M, Jezzard P, Woolrich MW. Separation of macrovascular signal in multi-inversion time arterial spin labelling MRI. *Magn Reson Med*. 2010;63:1357-1365.
86. Shirzadi Z, Stefanovic B, Chappell MA, et al. Enhancement of automated blood flow estimates (ENABLE) from arterial spin-labeled MRI. *J Magn Reson Imaging*. 2018;47:647-655.
87. Mutsaerts HJ, van Dalen JW, Heijtel DF, et al. Cerebral perfusion measurements in elderly with hypertension using arterial spin labeling. *PLoS One*. 2015;10:e0133717.
88. Tsujikawa T, Kimura H, Matsuda T, et al. Arterial transit time mapping obtained by pulsed continuous 3D ASL imaging with multiple post-label delay acquisitions: comparative study with PET-CBF in patients with chronic occlusive cerebrovascular disease. *PLoS One*. 2016;11:e0156005.
89. Dai W, Fong T, Jones RN, et al. Effects of arterial transit delay on cerebral blood flow quantification using arterial spin labeling in an elderly cohort. *J Magn Reson Imaging*. 2017;45:472-481.
90. Dolui S, Fan AP, Zhao MY, Nasrallah IM, Zaharchuk G, Detre JA. Reliability of arterial spin labeling derived cerebral blood flow in periventricular white matter. *Neuroimage Rep*. 2021;1:100063.
91. Iadecola C. Neurovascular regulation in the normal brain and in Alzheimer's disease. *Nat Rev Neurosci*. 2004;5:347-360.
92. Huang C, Mattis P, Tang C, Perrine K, Carbon M, Eidelberg D. Metabolic brain networks associated with cognitive function in Parkinson's disease. *Neuroimage*. 2007;34:714-723.
93. de la Torre JC. Cardiovascular risk factors promote brain hypoperfusion leading to cognitive decline and dementia. *Cardiovasc Psychiatry Neurol*. 2012;2012:367516.

SUPPORTING INFORMATION

Additional supporting information can be found online in the Supporting Information section at the end of this article.

How to cite this article: Thropp P, Phillips E, Jung Y, Thomas DL, Tosun D. Arterial spin labeling perfusion MRI in the Alzheimer's Disease Neuroimaging Initiative: Past, present, and future. *Alzheimer's Dement*. 2024;20:8937–8952. https://doi.org/10.1002/alz.14310